ELSEVIER

Nuclear Instruments and Methods in Physics Research A 491 (2002) 23–40

NUCLEAR INSTRUMENTS & METHODS IN PHYSICS RESEARCH Section A

www.elsevier.com/locate/nima

The superconducting inflector for the BNL g-2 experiment ☆

A. Yamamoto[a], Y. Makida[a], K. Tanaka[a], F. Krienen[b], B.L. Roberts[b], H.N. Brown[c], G. Bunce[c], G.T. Danby[c], M. G-Perdekamp[c], H. Hseuh[c], L. Jia[c], Y.Y. Lee[c], M. Mapes[c], W. Meng[c,*], W. Morse[c], C. Pai[c], R. Prigl[c], W. Sampson[c], J. Sandberg[c], M. Suenaga[c], T. Tallerico[c], F. Toldo[c], K. Woodle[c], M.A. Green[d], I. Itoh[e], H. Otsuka[e], Y. Saito[f], T. Ozawa[f], Y. Tachiya[f], H. Tanaka[f], A. Grossmann[g], K. Jungmann[g,1], G. zu Putlitz[g], H. Deng[h], S. Dhawan[h], V. Hughes[h], D. Kawall[h], J. Pretz[h], S. Redin[h], E. Sichtermann[h], A. Steinmetz[h]

[a] *KEK, High Energy Accelerator Research Organization, Tsukuba, Ibaraki 305-0801, Japan*
[b] *Boston University, Boston, MA 02215, USA*
[c] *Brookhaven National Laboratory, Upton, NY 11973-5000, USA*
[d] *Lawrence Berkeley Laboratory, Berkeley, CA 94720, USA*
[e] *Nippon Steel Co., Futtsu City, Chiba Pref. 293-8511, Japan*
[f] *Tokin Co. Sendai City, Miyagi Pref. 982-8510, Japan*
[g] *Universität Heidelberg, 69120 Heidelberg, Germany*
[h] *Yale University, New Haven, CT 06511, USA*

Received 24 May 2002; accepted 5 June 2002

Abstract

The muon g-2 experiment at Brookhaven National Laboratory (BNL) has the goal of determining the muon anomalous magnetic moment, a_μ (= (g-2)/2), to the very high precision of 0.35 parts per million and thus requires a storage ring magnet with great stability and homogeneity. A super-ferric storage ring has been constructed in which the field is to be known to 0.1 ppm. In addition, a new type of air core superconducting inflector has been developed and constructed, which successfully serves as the injection magnet. The injection magnet cancels the storage ring field, 1.5 T, seen by the entering muon beam very close to the storage ring aperture. At the same time, it gives negligible influence to the knowledge of the uniform main magnetic field in the muon storage region located at just 23 mm away from the beam channel. This was accomplished using a new double cosine theta design for the magnetic field which traps most of the return field, and then surrounding the magnet with a special superconducting sheet which traps the remaining return field. The magnet is operated using a warm-to-cold cryogenic cycle which avoids affecting the precision field of the

☆ Work was supported by the US Department of Energy and by the US–Japan Program for Cooperation in High Energy Physics.
*Corresponding author. Tel.: +1-631-344-2120; fax: +1-631-344-5954.
E-mail addresses: meng@bnl.gov (W. Meng).
[1] Present address: Kernfysisch Versneller Instituut, 9747 AA Groningen, Netherlands.

PII: S0168-9002(02)01232-9

storage ring. This article describes the design, research development, fabrication process, and final performance of this new type of superconducting magnet.

PACS: 42.20.G; 85.25.Ly; 85.70.Ay

Keywords: Muon g-2; Superconducting magnet; Accelerator magnet; Magnetic flux shielding; Applied superconductivity

1. Introduction

In the 1970s, a CERN g-2 experiment [1] achieved the precision of 7 parts per million (ppm) on the measurement of the muon anomalous magnetic moment. The result agreed well with theoretical expectations from the electromagnetic and strong forces, and placed stringent limits on theories involving new physics processes. The present muon g-2 experiment at Brookhaven's Alternating Gradient Synchrotron proposed to reach a factor 20 greater precision, which would then show the effects of the weak interaction contributions to the muon g-2 value, and probe for new physics at a multi-TeV scale. In order to improve the precision of the measurement by the factor 20, the BNL g-2 experiment (E821) had to significantly reduce the systematic errors from the CERN experiment, including the uncertainty in the value of the storage ring magnetic field. The goal is to know the field, averaged around the storage ring, to 0.1 ppm. This goal was recognized as possibly the greatest difficulty to overcome for a successful experiment.

The experiment decided to use 3.1 GeV/c muons for the measurement, to take advantage of the "magic" energy where the muon spins are not affected by electrostatic focusing, which is then used to keep the muons stored. This energy, and the decision to use iron to shape the storage ring magnetic field, determined the required field and radius for the storage ring. A super-ferric muon storage ring magnet with a radius of 7.11 m and a field of 1.45 T has been constructed [2], which provides a uniform magnetic field in the muon storage region, a 90 mm diameter toroid with 7 m radius. A high-precision-pulsed NMR system has been developed and built [3] which measures the field to 0.1 ppm.

The injector magnet, described here, must allow the muons, collected in an external beam line from pion decays, to enter the storage ring aperture, at a small angle so that a special pulsed magnetic field in the storage ring aperture, from a separate "kicker" magnet, can then kick the muons onto stable orbits. (For the first stage of the Brookhaven National Laboratory (BNL) experiment, pions from the beam line were brought into the storage ring, and a small fraction of pions which decayed in the storage aperture resulted in stored muons; no kicker magnet was used. This "pion injection" technique was used also for the CERN experiment.) The required bending angle of the injector, which cancels the main field locally, is 0.25 rad, and the required kick of the pulsed kicker magnet is 10 mrad. The injector field must be very close to the storage ring, but must not spoil the knowledge of the storage ring field at a 0.1 ppm level.

The injection of a particle beam into a storage ring is usually done with a pulsed magnetic inflector (which plays the roles of "injector" and "deflector"). It locally cancels the main magnetic field, so that the beam enters the storage region over as short a path as possible, and almost tangent to the equilibrium orbit of the ring. The short path length is required to minimize defocusing effects on the entering muons from the fringe field of the storage ring. In the CERN g-2 experiment, a copper coaxial structure pulsed inflector was used. The skin depth of the copper determined the initial magnitude of the pulse, which propagated as a wave away from the device. In the CERN storage region, the fringe field from the pulsed inflector was time dependent: it had the magnitude of several hundred gauss at 1 μs and decreased to about 20 G at 600 μs, the time when data collection ended [4].

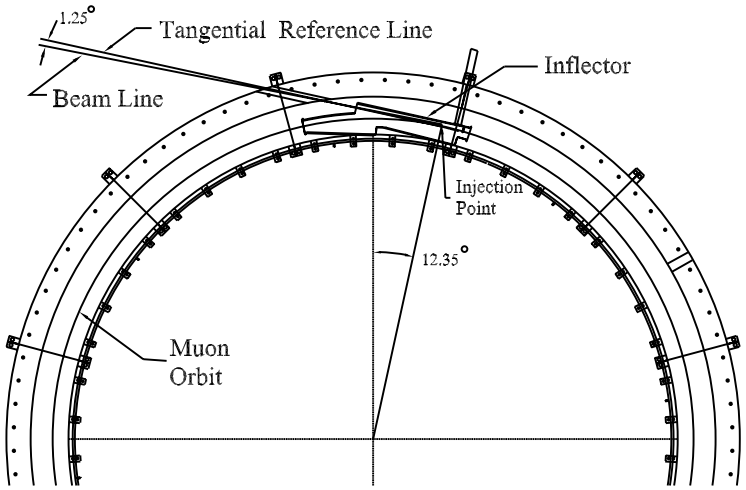

Fig. 1. Inflector in the storage ring.

Fig. 1 shows a schematic layout of the present inflector in the BNL g-2 storage ring. To satisfy the needed precision of the storage ring magnetic field, the requirements of the BNL g-2 inflector were well defined. (a) It must create enough integral field (2.6 T m) at the entrance of the ring, to give an 0.25 rad kick to the 3.1 GeV/c incoming (pion/muon) beam. (b) It must have very limited influence on the field uniformity. Here, "limited" means that it must not affect the storage of coasting muons, and it must not degrade the measurement precision (0.1 ppm) in the 45 mm radius toroidal storage region. The radial distance between the injection line and the muon storage equilibrium orbit is only 77 mm, in order to maintain a high muon capture ratio.

Three options were studied for such a device: (1) a pulsed CERN-type magnetic inflector; (2) a flux exclusion tube; and (3) a direct current iron-free magnetic inflector.

In considering option (1), for the BNL g-2 experiment each of 12 RF bunches is fast-extracted, separated by 33 ms, per AGS cycle ($\sim$2.8 s); while in CERN's case, beam was extracted once per 2.3 s PS period. After consideration of the material heating and stress, and the required solid state switches and ignitrons under such high repetition rate for the BNL experiment, it was concluded that a pulsed inflector would be very difficult to accomplish regardless of the uncertainty of the time variation of the fringe field [5].

Option (2) would use a superconducting tube to exclude the main storage ring magnetic flux along the injection line. In order to prevent the 1.45 T field from entering the beam tube, the Eddy current generated on the outer surface of the tube must be significant, and these large currents would also affect the main field uniformity in the muon storage region. Fig. 2 shows the computer simulation of the diamagnetic property ($\mu_r \ll 1$) of the superconducting material. The flux lines of the storage ring are repelled by an oblong superconducting tube and the distortions are readily apparent. The maximum field disturbance in the muon storage region (shown by a dotted semicircle) could be as large as 10% (or 100,000 ppm).

Option (3) was chosen by the g-2 collaboration: a direct current non-ferrous superconducting septum magnet. A double cosine theta design provides a 1.5 T field close to the storage region, and traps its own fringe field, with a small residual fringe field remaining. Studies of using iron shimming to correct for this residual field were not successful, but the design goal was finally achieved with an additional superconducting

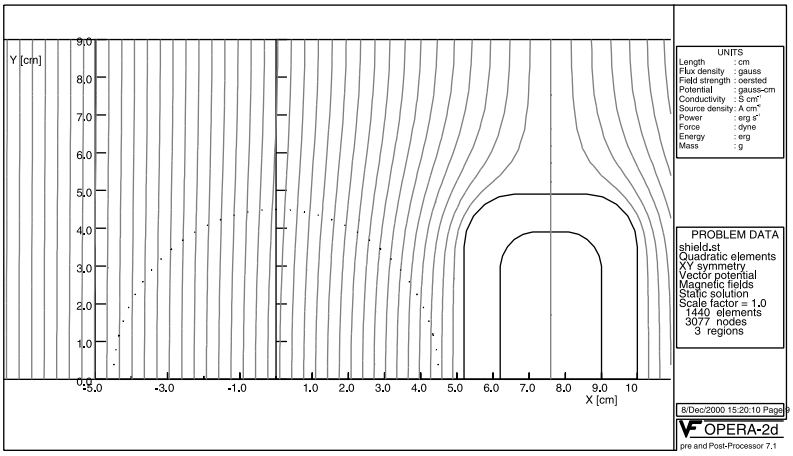

Fig. 2. Flux exclusion tube (simulation).

shield, which traps (or shields) only the residual fringe field, instead of the main magnetic flux as suggested in option (2). This device fits in between the poles of the storage ring and does not influence the knowledge of the storage ring field, integrated around the storage ring, at the 0.1 ppm level.

2. Conceptual design

The conceptual design of the g-2 inflector was based on the truncated double cosine principle. Ref. [6] describes this method in detail, from the complex potential theory, to the formulas which can be used to shape the N-pole field, reducing the fringe field in generic air-core magnet designs. It is useful to emphasize a few key points, which have been developed beyond the original cosine theta theory [7]:

(A) The double cosine principle offers options to superimpose any N-pole current density in the complex potential formula, which results in shaping the field component at will, and allows optimization of the return flux to a desired configuration.

(B) Truncation is invariably along a constant vector potential line. It offers the option to use only part of the field generated by the N-pole current density. This is achieved by placing the computed line current on truncation boundaries. As long as the applied current is equal to the scalar potential difference between adjacent wires, it will nullify the field outside the boundary but leave the field inside unchanged.

The above features make this design different from other "self-contained flux magnets": the useful field region is maximized, and the number of total ampere-turns are minimized. Fig. 3 shows only the upper half of the final conceptual design: line current distribution and flux. The current density around the circle ($R = 50$ mm) essentially obeys the cosine theta distribution, except that certain wires were re-arranged near the intersect boundaries. The truncation along the straight line $x = 15$ mm, followed by an arc crossing at $x = 93$ mm, is one of the constant vector potential A lines, along which the truncation occurs. The uniform dipole field region (beam channel) lies between $x = 15$ and 45 mm. The return flux region (between $x = 55$ and 93 mm) has been compressed by a factor of 2, compared with the natural return flux in a single cosine theta design. This is achieved by applying a virtual current density, which is also a cosine theta distribution but in the opposite direction. This virtual current is not present explicitly, but actually squeezes the return flux, so that the ratio of the useful field region is optimized, and the overall cross-section area is reduced to fit the limited space between the muon channel and the main magnet coils

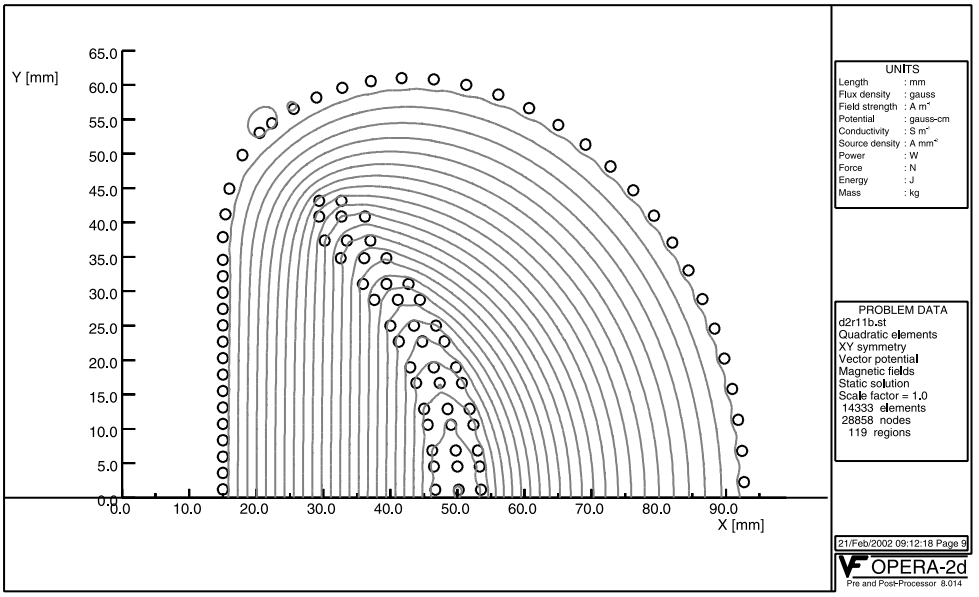

Fig. 3. Conceptual design.

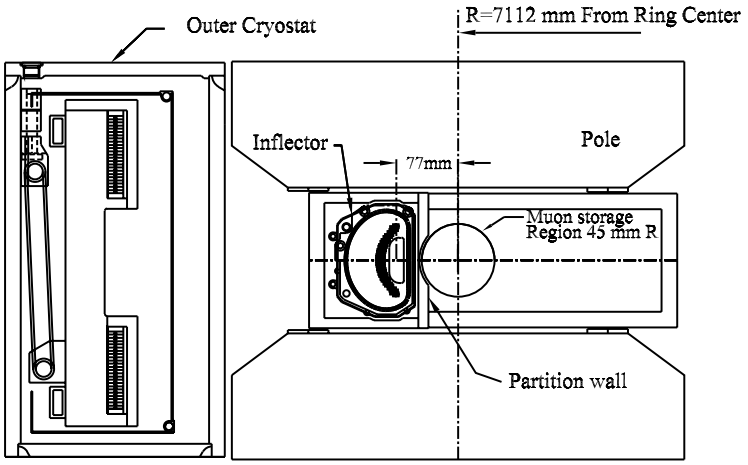

Fig. 4. Inflector at injection point.

(Fig. 4). Here, the trade off is to apply 10% more current density on the $R = 50$ mm arc (compare this with the single cosine distribution case). The design current was 2850 A (88 turns), to provide 1.5 T field in the beam channel, which is able to cancel the integrated main field, and guide the incoming beam along the inflector beam channel [8,9].

3. Research and development

Aluminum-stabilized superconductor was chosen for the BNL g-2 inflector: (a) to minimize the interactions of the incoming pion/muon beam at both upstream and downstream ends of the coil with no open apertures for the beam, and (b) to make the coils and cryostat design compact, so

that the conductive cooling (without liquid helium containers surrounding the coils) can be achieved effectively.

An existing Al-stabilized superconductor was supplied by Japan KEK (fabricated by Furukawa Co.). This conductor was developed for ASTRO-MAG (Particle Astrophysics Magnet Facility) [10,11]. Fig. 5 shows the cross-section of this conductor. The basic parameters are listed in Table 1.

From computer calculation, the peak field seen by the inflector conductor filaments reaches 3.5 T, if the self-field effect [12] is taken into account. This is due to the superposition of the return flux and the main field. Short sample tests were performed at KEK and BNL. The results showed that the critical current of this superconductor is about 3890 A at 4.6 K and 3.5 T. In the g-2 storage ring, the inflector sees 1.45 T field (from the main magnet) even at zero operating current. From the conductor characteristics, the inflector operates at around 73% of the full load (at 4.6 K). The short sample test data and the inflector load line (in the storage ring field environment) are shown in Fig. 6.

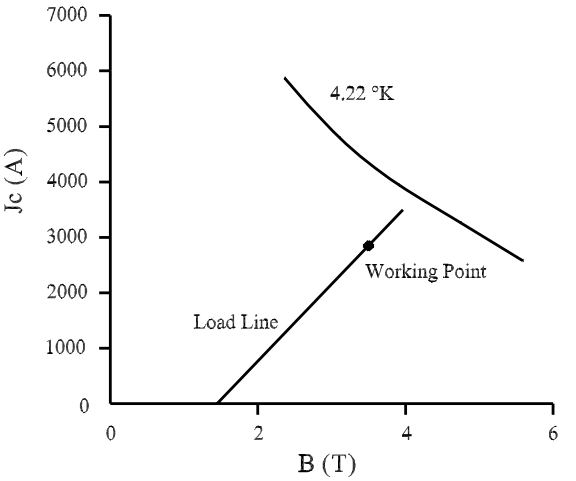

Fig. 6. Superconductor characteristics and the inflector load line in the environment of 1.45 T magnetic field.

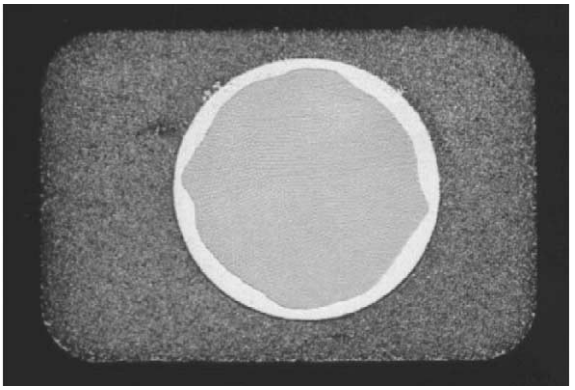

Fig. 5. Cross-section of the aluminum stabilized superconductor.

Table 1
Parameters of conductor (ASTROMAG/g2inf)

Configuration (NbTi:Cu:Al)	1:0.9:3.7
Stabilizer	Al (99.997%); RRR = 750
Process	Co-extrusion
NbTi/Cu composite	Diameter 1.6 mm (monolith)
NbTi filament	Diameter 0.02 mm
Number of filaments	3050
Twist pitch	31 mm
Conductor dimension	2×3 mm
Insulated conductor dimension	2.3×3.3 mm

Research and development for the superconducting inflector magnet began in 1989 at KEK in conjunction with Tokin Corporation.

The first step in developing an engineering design for such a complicated magnet was to determine a suitable dividing line to separate the magnet into two coils. The considerations were to reserve the beam channel to one coil, to reduce the complexity of the end loops, and to make the assembly process less difficult after two coils are wound separately. Fig. 7 shows a cross-section view of the coils and the optimized dividing line in the engineering design. The symbols $\times$ and $\bullet$ in the conductors represent the different current directions.

End winding configurations were extensively studied by using dummy and real conductors [13]. Fig. 8 shows two options. The open-type option leaves the beam channel clear, but end loop support and constraint is much more difficult. The closed-type option forces the incoming beam

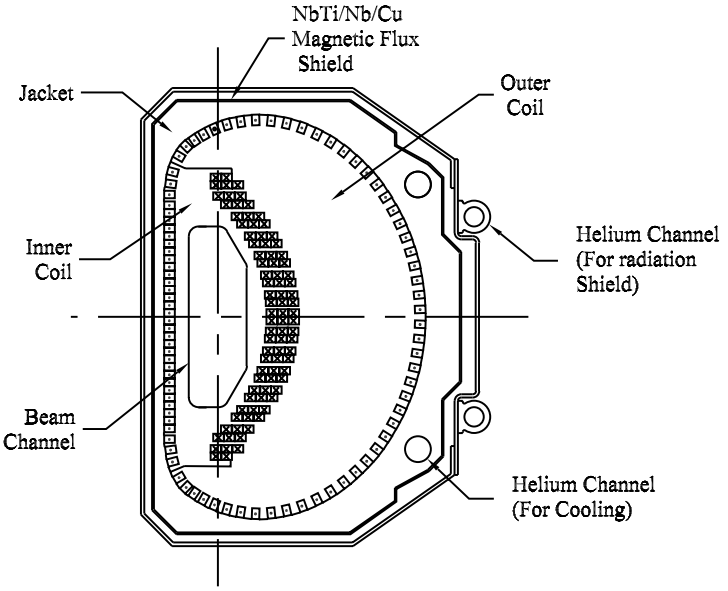

Fig. 7. Inflector cross-section.

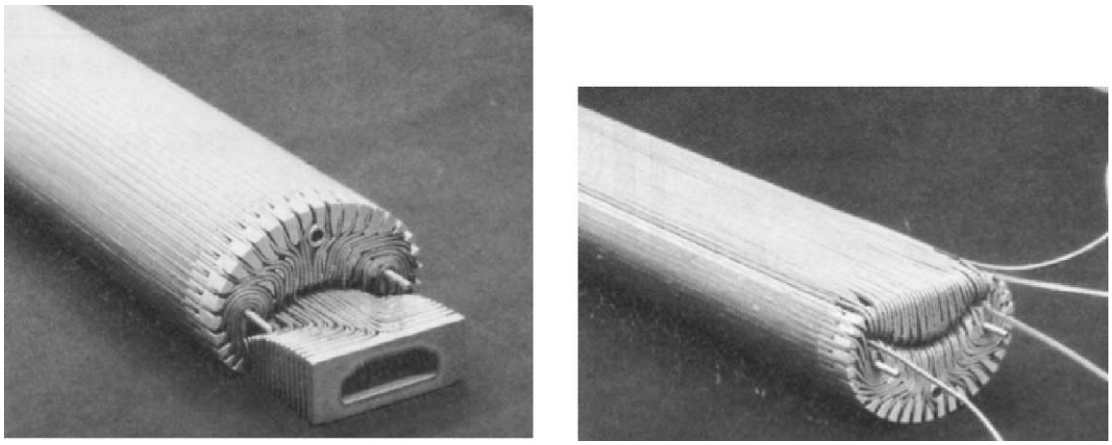

Fig. 8. End options.

to penetrate conductor layers, resulting in multiple scattering, but provides much better mechanical and cryogenic stability, and occupies less physical space. Later studies also showed that the closed-type option gives much less fringe field. A third option, with the upstream end open and the downstream end closed, was also discussed. In that case, the muon storage efficiency would not increase significantly, while the engineering difficulties would remain [2]. The second option, with both ends closed, was chosen.

The outer coil has many more turns (52 turns) than the inner coil (36 turns). A difficulty in stacking the end layers for the outer coil was solved by using a double-layer winding scheme. For the first layer, only every other turn was

[2] E821 Design Report, BNL

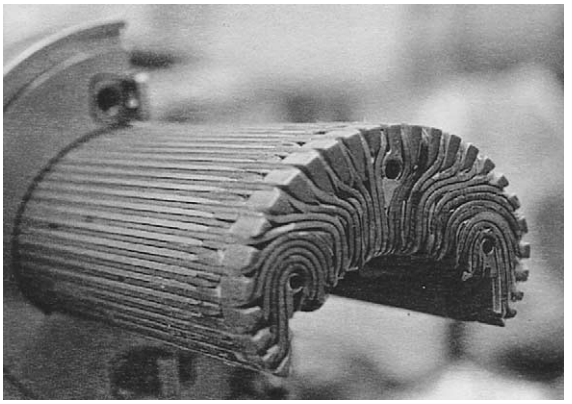

Fig. 9. Outer coil end (double layer).

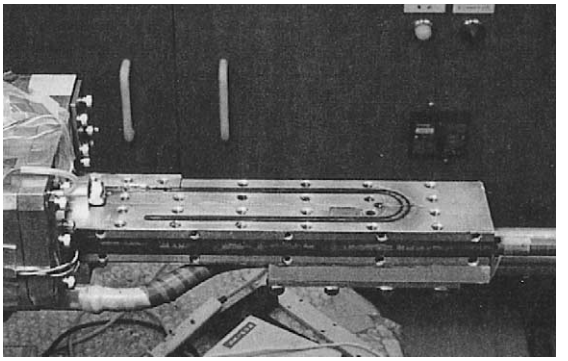

Fig. 10. Joint and lead holder.

wound on the mandrel. After applying a special outer coil end cap, the remaining turns were then wound and the second layer was formed, as shown in Fig. 9. This configuration keeps end-loops inside machined grooves, and ensures sufficient mechanical constraint and heat conduction.

An aluminum case was designed to serve the following functions: (1) to constrain the conductors along the 1.7 m long surface; (2) to provide sufficient cooling through machined liquid helium paths.

The inner coil and the outer coil are connected in series. The joint is located inside the downstream end of the coils; and is made by soldering the superconductors without removing the aluminum stabilizer. The joint resistance is less than 10 nΩ at 3000 A and 4.2 K. The joined leads were placed inside a U-shaped groove, as shown in Fig. 10, attached to the coil end structure. Cooling tubes run through the extender (aluminum block). One temperature sensor was mounted near the joint to monitor the local ohmic heating.

The electric power leads also pass through this extender. The same type conductors are used as additional stabilizer to enhance these leads. The lead holder and cover were designed to resist the Lorentz force due to the external main magnetic field, and to make good contact with the cooling tubes.

Prior to the inflector fabrication, a superconducting prototype was developed, with full sized cross-section and shortened length (magnetic length 500 mm). It was energized at KEK with zero external field in 1993 [15], and at BNL with 1.45 T external field in 1994 [16]. During these prototype superconducting magnet tests, no training phenomena were observed. Quenches were induced by using a fast ramp rate, stopping the cryogen flow, and using an internal heater. The data for the temperature margin, measured load line, and quench velocities were studied. The fringe field and superconducting shield were also studied using this prototype, and will be discussed in Sections 4 and 5.

The very successful prototype tests established an important milestone, which indicated that the major difficulties had been overcome.

Based on the experiences of the prototypes, the fabrication of the full-scale inflector then

Table 2
Parameters of the superconducting inflector

Overall dimension	110(W) × 150(H) × 2025(L) mm
Magnetic length	1700 mm
Beam aperture	18(W) × 56(H) mm
Design current	2850 A (with 1.45 T main field)
Number of turns	88
Channel field	1.5 T (without main field)
Peak field	3.5 T (at design current, with main dipole field)
Inductance	2.0 mH
Resistance	1.4 Ω (at 300 K)
Cold mass	60 kg
Stored energy	9 kJ (at design current)

began. The design parameters are shown in Table 2.

4. Residual fringe field

Once we use the principle described in Section 3 to design a physical double cosine theta winding, individual wires must replace the ideal continuous surface current density. The wire size in Fig. 3 is the exact size of the NbTi/Cu core in Table 1. Because the current density is discrete, the field outside the truncated boundary is no longer zero but has a finite magnitude. In the conceptual 2D design, this field was less than 10 G, or 700 ppm (see footnote 1). This was consistent with the measurement on a powered wire model as long as the probe was far away from both ends [14].

Once the coil winding was complete, the effects of the ends needed to be considered. As discussed in Section 3, the closed end option gives much less fringe field. Furthermore, once the winding becomes superconducting, the following effects give possible additional sources of fringe field:

(1) Slight variations of the location of the superconducting core. The center of the conductor could vary by up to a few tenths of a millimeter.

(2) Mechanical tolerance on the mandrels: The conductor was insulated by formvar and fiberglass tape, then wound into the machined grooves on the coil mandrels. Winding, assembly, and epoxy resin curing also affect the mechanical tolerances. The tolerance of the superconductor positioning directly affects the field quality.

(3) *Magnetization effect*: During the current ramp, Eddy currents are induced inside each filament. The dipole effects are de-coupled by the "twist pitch" of the filaments in the composite [17], but high-order multipoles could still influence the internal (beam channel) and external (storage region) magnetic field.

Fringe field measurements were made on the superconducting prototype at room temperature with 20 A current, and at superconducting temperature at full nominal current. The resulting fringe field measurements were consistent [18]. These suggest those sources (1) and (3) are not important. Further detailed computation showed that the magnetization effect, source (3), in the muon storage region is quite small (less than 70 ppm) [19]. Source (2) is the dominant origin of the residual fringe field.

At the design current, the maximal fringe field within the muon storage region was about 200 G (1.4%) near the outer edge. The fringe field behaves in such a way that it is a rapidly varying function along the transverse direction, i.e. the radial direction of the storage ring, and essentially gives a negative disturbance. The fringe field of the inflector (prior to the addition of the superconducting shield) is opposite to the main field at the outer radius of the storage ring, and changes sign while crossing the central orbit.

The consequence of such a fringe field is severe. The high gradient of the field would be beyond the working range of the NMR probes, so that the magnetic field map of the storage region would be incomplete, directly impacting the error of the measurement precision of the muon magnetic moment. Special measurements in this region are possible, by using Hall probes, or, by varying the NMR reference frequency, trigger time, and excitation amplitude. These methods may reduce the error on the field value, but on the other hand, would introduce an enhanced position error due to two independent field maps, which must be corrected. The residual fringe field had to be further reduced in order to reach the final goal of the g-2 experiment.

Conventional magneto-static shimming studies to reduce this fringe field were begun, using computer simulations. The iron compensation must be located outside the muon storage region. Its contribution to the central field will be a slowly varying function in this space, which is not able to cancel the larger gradient fringe field to an acceptable level [20].

The best way to eliminate a multipole fringe field is to create an opposite mulipole current source with the same magnitude. The best such current source is the super-current generated inside a superconducting material due to the variation of the surrounding field. A method of using SC material to shield the inflector residual fringe field was studied and developed. The fringe field specification was then satisfied.

5. Superconducting shield

In addition to the disappearance of electric resistivity, superconductivity has a second characteristic: diamagnetism. For type I superconductor, it is known as the Meissner effect, which shows not only that a magnetic field is excluded from a superconductor, but also that a field is expelled from superconducting materials originally in the normal state, as it is cooled through the transition temperature T_c, provided $H < H_c$. For type II superconductor, the Meissner effect exists only if $H < H_{c1}$. In the range above H_{c1}, it is known as a mixed state rather than the ideal superconducting state. Its behavior in the magnetic field is just like a "perfect conductor": it simply opposes any changes of the flux density by generating an internal Eddy current, provided $T < T_c$ and $H_{c1} < H < H_{c2}$. This current is very much like the Eddy current described by Faraday's Law of Induction and Lenz's Law, except that it does not decay, but remains at a constant density J_c, the critical current density. The type I material is not useful for magnet-grade application due to its low H_c. The high H_{c2} of type II material, which made superconducting magnets possible, and its field history "memory" just fit the requirements for the inflector.

In a previous application [21], the goal was to exclude 1.5 T field by using a lead–tin soldered multi-section Nb_3Sn tube, which had no concern for external field distortions. A "field-free region" was created with 3.72 mT (or 2500 ppm) residual field at the center of each tube section. Our strategy was to reserve the original role for the inflector, but only use the superconducting shield to prevent the inflector fringe flux from leaking out to the muon storage region. Therefore, much less distortion (in the channel field) and much better extinction rate (in the stored muon region) were required and expected.

The ideal location of the superconducting shield is on the outer surface of the inflector coil case (Fig. 7). The inflector must stay above the transition temperature T_c when the storage ring magnet is energized, so that the flux of the main magnetic field penetrates the superconducting shield, which is in the normal state. After the main field reaches its stable level (1.45 T), one may cool down the inflector together with the superconducting shield to liquid helium temperature. In this step, the ambient field (1.45 T) already exceeds H_{c1} (0.009 T for NbTi), and therefore the Meissner effect does not hold, or in other words, the main flux is not repelled. It is then time to energize the inflector at the proper ramp rate. On one hand, the superconducting shield traps the flux of the main magnet; on the other hand, as the inflector current increases, its fringe field increases; dB/dt induces Eddy current in the superconducting shield, which tends to keep the fringe flux from entering the interior of the shield material. The fringe flux lines are effectively "pinned" around the inner surface of the shield. According to the critical state model [22], the Eddy current density equals the critical current density of the shield J_c. The minimal thickness of the shield d needed to completely block the fringe field is: $d = B/\mu_0\ J_c$, where J_c is a function of field and temperature.

The first superconducting shield test was performed in 1993 in order to confirm the above proposal. Fig. 11 shows the cross-section of the setup. A NbTi plain sheet ($J_c = 100\ A/mm^2$ at 1.5 T, 4.2 K) surrounded a superconducting SSC sextupole magnet. On the sheet surface, a stainless steel ribbon was wrapped as a heater, which controls the temperature of the sheet. Two Hall

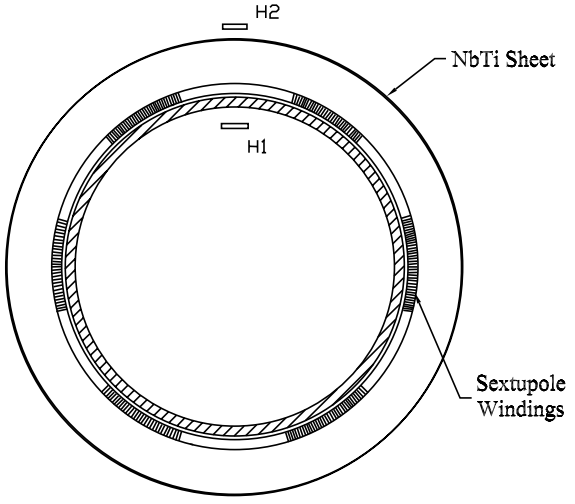

Fig. 11. Shield test on SSC sextupole.

probes H1 and H2 were monitoring the magnetic flux densities inside and outside of the sheet, respectively. The whole system was placed in a liquid helium dewar. Flux shielding and trapping is exhibited in Fig. 12. Whenever the heater is on, the sheet is normal, and H2 sees the leakage field directly proportional to the magnet current ($\sim$3.2 G/A). Whenever the heater is off, the sheet is in the superconducting state, and keeps the field value at the transition moment. As horizontal lines show in the figure: if the magnet current increases, then it shields the extra field; if the magnet current decreases, then it traps the previous field. This test clearly demonstrated the type II superconductor's "perfect conductor" property, and verified that the superconducting shield application is feasible.

It was reported that much higher J_c NbTi/Nb/Cu multi-layer composite sheet (or tubes, cups) was developed at Nippon Steel Corporation. The sheet contains 30 layers NbTi, 60 layers Nb, and 31 layers Cu. The Cu layers greatly improved the dynamic stability against flux jumping [17]. The Nb layers act as barriers, which prevent the diffusion of Ti into Cu. The diffusion could form hard inter-metallic layers and create difficulties for the rolling process. Fig. 13 shows the typical cross-section of the sheet. Detailed information and the fabrication procedure are described in [23]. This type of sheet was ideal for the requirement of the inflector shield. A special thin sample sheet was then developed at Nippon Steel Corp. The measured overall critical current density was above 500 A/mm^2 (at 1.5 T, 4.2 K, H$\perp$ NbTi layers). The critical current density J_c of NbTi was about 1200$\sim$1400 A/mm^2 (at 1.5 T, 4.2 K, H$\perp$NbTi layers), and above 2000 A/mm^2 (at 1.5 T, 4.2 K, H $\parallel$ NbTi layers).

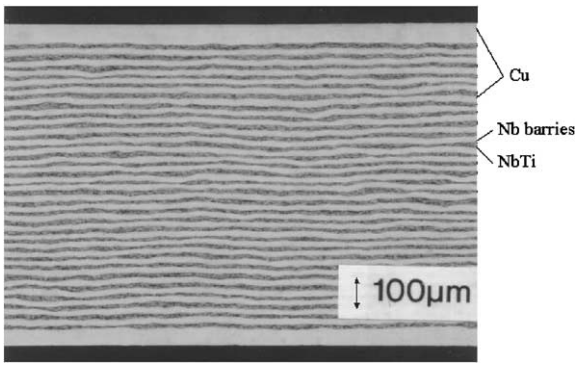

Fig. 13. Cross-section of the multilayer sheet.

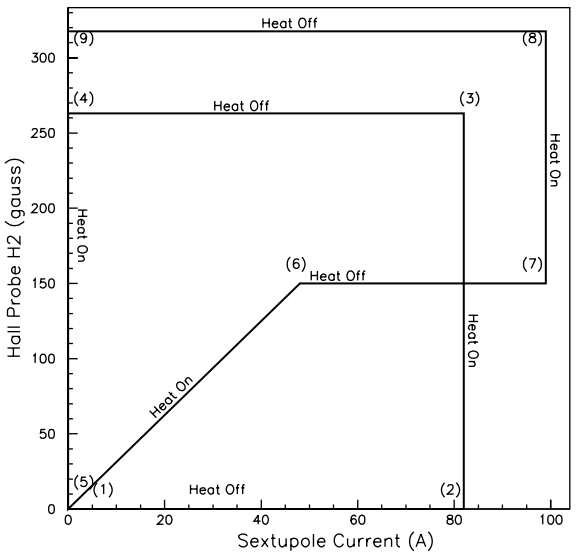

Fig. 12. "Perfect conductor" property of NbTi.

A second superconducting shield was tested in 1994, on the prototype inflector which was discussed in Section 3. The shield was made by a small piece of multilayer composite sheet (with thickness of 0.5 mm), which was formed as a sleeve, and glued by epoxy on the downstream part of the prototype. A special cryostat chamber was made to simulate the confined space located around the injection point (as shown in Fig. 4), and was placed inside a dipole magnet (AGS type 18D72), which provided the same field (1.45 T) as the g-2 storage ring. Shielding effects with and without the external magnetic field were studied [24,25]. This test verified that the heat radiation and flux jump would not be problems, under the indirect cooling system and the slow ramp rate.

Based on the above successful tests, Nippon Steel Corp. developed large, thin pieces of sheet especially for the g-2 inflector, to cover its 2 m $\times$ 0.5 m surface and to fit into the limited space between the storage region and main magnet coil. The shielding result was extremely satisfactory.

6. Superconducting inflector fabrication

The inner coil was wound on the beam bore tube, which functions also as a mandrel (one-layer winding). The outer coil was wound on the outer coil mandrel (two-layer winding), by applying additional end caps between the layers, as described in Section 3 and Fig. 9. The material of the mandrels is 6061 aluminum alloy. The same material was used for precise spacers to fill in gaps between the end turns (Fig. 14).

After the two coils were assembled, they were wrapped with electrical insulation layers (kapton), and then inserted into the pre-heated aluminum case.

The case was equipped with helium cooling path (aluminum tubes). Epoxy resin was impregnated at 50°C under vacuum, and cured at 120°C and 0.5 atm/cm^2 pressure. Up to this step, the physical length was 1.7 m, equivalent to the defined magnetic length (Fig. 15).

On the downstream flange surface, grooves were machined. The two leads were laid next to each other, following the "power leads groove"; another two leads were soldered together and insulated, sited along a U-shaped groove, forming the intermediate joint (Fig. 16). The entire lead holder was designed to achieve the following goals: rigid mechanical constraint, sufficient cooling, reliable electric insulation, and least fringe field (Fig. 10).

Including the lead holder (downstream extender), the total length then became 2.025 m. After surface preparation, the superconducting shield was formed and glued on the outer surface of the entire body by using epoxy resin (Fig. 17). In the final version, the thickness of the shield is 0.5 mm.

Before the installation of the thermal radiation shield, which is also made of aluminum, multi-layer super-insulation was loosely wrapped around the magnet, and then a PTFE tube string was wound spirally, in order to keep 3 mm clearance between the magnet and the radiation shield (Fig. 18).

In KEK tests, liquid nitrogen (77 K) was used as the radiation shield cryogen; in the BNL test and physics operation, helium vapor ($\sim$30 K) has been used. Thermal anchors were applied to provide cooling paths between the cryogen and critical

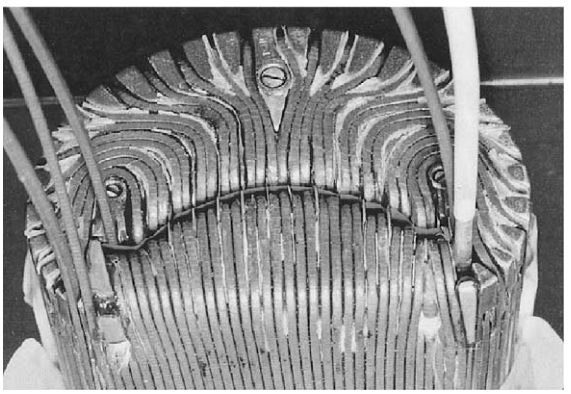

Fig. 14. Down-stream coil spacers.

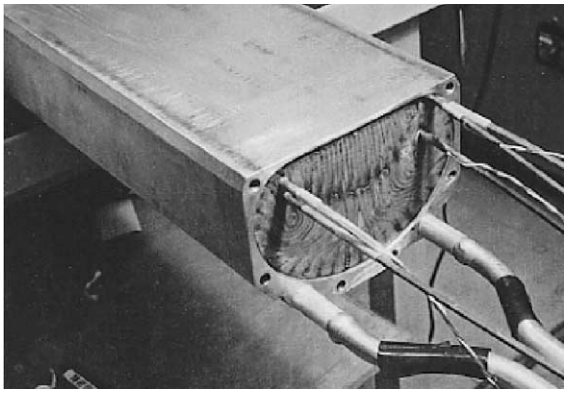

Fig. 15. After impregnation and curing.

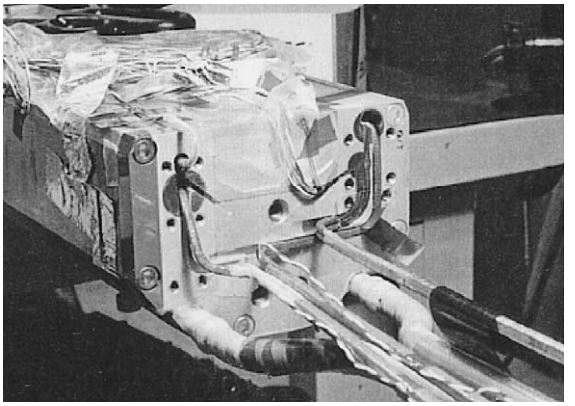

Fig. 16. Down-stream flange installation.

portions, such as magnet support legs, joint block, etc.

Two types of sensor are used to monitor the magnet temperature: CGR (Lake-shore Corporation) and Pt-Co (Chino Corporation). Both are resistor-type, and therefore insensitive to the magnetic field. The former works well in a low-temperature range; the latter works well in a high-temperature range. Hall sensors (Siemens Corporation) were installed inside the beam channel to monitor the magnetic field on the incident muon beam.

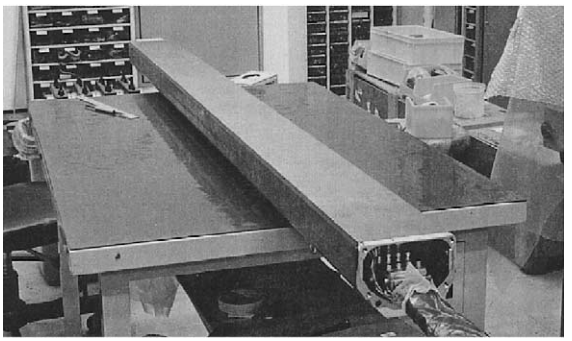

Fig. 17. Superconducting shield (installed).

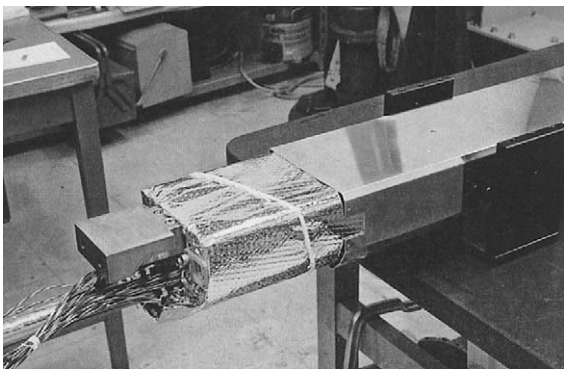

Fig. 18. Thermal radiation shield installation.

7. Cryostat design

The injection beam line is set to a 1.25° angle from the tangential reference line (Fig. 1). The inflector is aligned along this reference line and its downstream end is positioned at the injection point. The point where the reference line is tangent to the storage ring circumference is 77 mm radially from the muon central orbit. The main magnet fringe field, upstream of the inflector, bends the incoming beam by about 1.25°, so that the beam enters the inflector nearly parallel to the inflector axis. The inflector cryostat and one of the storage ring beam vacuum chambers were designed as an integral structure, but with two separate vacuum zones. It is an aluminum structure with all joints welded for vacuum integrity. Fig. 19 shows its interface with the main magnet outer coil cryostat and how it connects into the muon vacuum chamber system.

The required functions and limited space challenge the design. At the downstream end (Fig. 4) where the inflector is very close to the

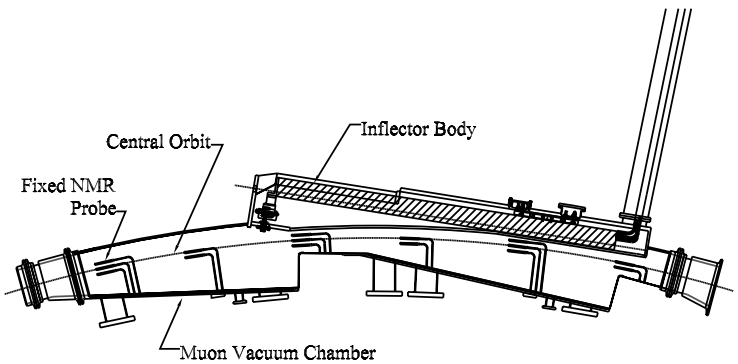

Fig. 19. Top view of cryostat and muon chamber.

storage region, a thin partition wall was designed to separate the inflector cryostat vacuum (10^{-5} mbar) from the muon beam vacuum (10^{-7} mbar). In the curved middle section, this wall was machined to 1 mm thickness to provide the required clearance for coasting muons but to still provide enough strength to sustain the pressure in the event that either side of the wall would lose vacuum. On the muon side, a groove was precisely machined on the wall to serve as part of the rail system for a device which carries 17 NMR probes inside the storage ring vacuum. At the upstream end (Fig. 20) where the inflector cryostat reaches into the main magnet outer coil cryostat, a concave indention was designed into the outer cryostat wall and two 45° chamfers were cut on the main magnet coil cover. This arrangement provides the needed space for a steering adjustment of up to 0.004 rad.

The inflector was installed into the cryostat through a rectangular (1156×145 mm) opening. The inflector is supported at two ends. The downstream end support was designed as a pivot so that the inflector exit coincides with the injection point. The upstream end support was designed as a slide to have both radial and tangential freedom to provide steering adjustment for the best muon storage ratio and to compensate for the shrinkage during the inflector cool down process. Also, these two short supports act as thermal insulators to keep the inflector at superconducting temperature, while the cryostat is at room temperature (300 K). Hybrid materials (G10 and aluminum) were used to reduce the heat conduction and to provide strength to sustain the Lorentz forces due to the main field, and during possible quenches. The total heat load from the supports was estimated to be 0.5 W. Due to limited space at the partition wall, only five layers of super-insulation were loosely wrapped outside the thermal radiation shield. The total heat load of the inflector (not including the vapor-cooled leads) is less than 13 W.

8. Cryogenic system

The g-2 main magnet and the inflector are cooled by one cryogenic system (with separate controls): a 625 W Claude cycle refrigerator system, which is equipped with a 1000 l control dewar to provide two-phase helium. System details were described in Ref. [26].

A special valve was designed to control the state of the inflector, in order to permit the necessary thermal cycling from warm-to-cold of the superconducting shield. The typical time required to warm up the inflector (> 10 K), letting main flux

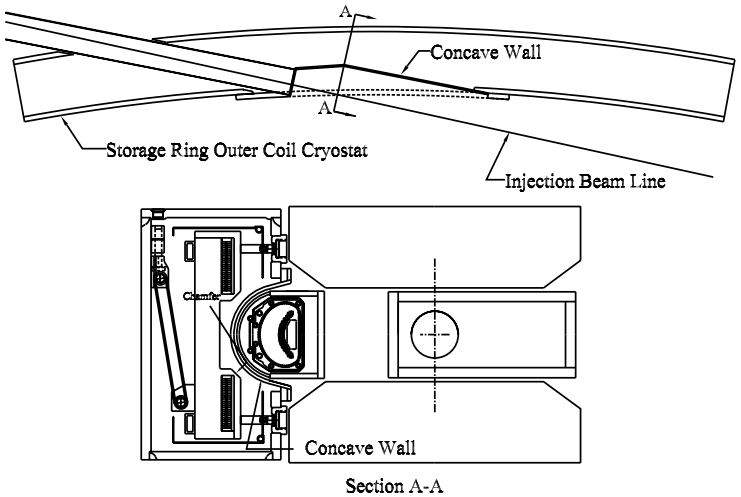

Fig. 20. Up-stream of cryostat and main magnet coils.

penetrate the shield, and then to cool down to the operation temperature (<5 K) is of the order of 30 min.

9. Power supply, power leads, and quench protection

The inflector power supply is a modified Transrax product, which was used for conventional magnets at BNL. It is driven by a 3-phase 480 V AC source, to provide a DC output (6 V, 3000 A). A water-cooled filter circuit was designed to reduce the current ripple to the 10^{-4} level. Additional interlocks were designed to match quench protection requests. The current ramp at the desired slow speed was achieved by an electronic circuit, which includes an analog function generator controlled by a simple circuit consisting of diodes, resistors, switches, and a 9 V battery. This control unit provides all options that are needed, such as variable ramping (up or down) speed and holding the operation current at any constant level. The typical ramp rate used is 2 A/s.

Tubular helium vapor-cooled electric power leads were designed [27] to make the transition from warm power cables to cold superconducting wires. This type of lead has a good temperature margin in case the cryogen flow stops accidentally.

Quenches are mainly detected by monitoring the voltage difference between the inner coil and the outer coil (with a certain weighted ratio). This threshold is set at 120 mV. Other voltage signals (such as lead voltage, intermediate and interconnection joint voltage) are also able to trigger the protection circuit to switch off the power supply. Since the total stored energy (9 kJ) is relatively low, the self-inductance is small (2 mH), and the quench velocities ($V_L = 100$ m/s, $V_T = 0.16$ m/s) [16] are quite high, the usual dump resistor is omitted.

10. Performance of the inflector magnet

The first full-scale g-2 inflector was tested in 1997 [28]. It was successfully used as a robust injection device for the g-2 data collection during three runs of AGS proton beam: 1997–1999.

The final (second) inflector was built with some improvements. The superconducting leads were combined inside of the downstream extender (see Section 6), which reduces the fringe field. The intermediate joint was built as a normal joint (without removing the aluminum stabilizer but with sufficient cooling path) to increase stability. The superconducting shield was constructed from two full-length pieces; one wide piece covers the entire flat surface facing the muon region, and overlaps with another piece on the back (farther from the muon region) of the coil case. This new superconducting shield improves the shielding effect.

This final inflector was first tested at KEK in 1998 without the external field. It experienced four training quenches, then reached 3000 A. The intermediate joint resistance was measured as $2 \times 10^{-9}\ \Omega$, and the temperature was very stable. There were no further training quenches in the second thermal cycle within the excitation range (3000 A).

This inflector was transported to BNL, and installed into the g-2 storage ring to replace the first one. After cool down, the temperature was measured to be below 5 K in the magnet, and around 30–50 K in the radiation shield. With the full external field 1.45 T from the storage ring, the inflector reached the design current 2850 A after one training quench (at 2560 A) Fig. 21. The magnet performance has been quite stable since December 1999. This inflector was then used for the g-2 runs in 2000 and 2001. The optimum current for injection was found to be 2724–2750 A, giving the best muon storage ratio. The superconducting performance of this magnet is fully satisfactory.

The fringe field from the inflector was examined by 17 NMR probes, which were mounted on a cable-driven trolley inside the storage ring vacuum region. All probes were able to measure the field throughout the inflector region at the standard reference frequency and time sequence for the g-2 field measurements, so that the field was completely mapped to 0.1 ppm precision.

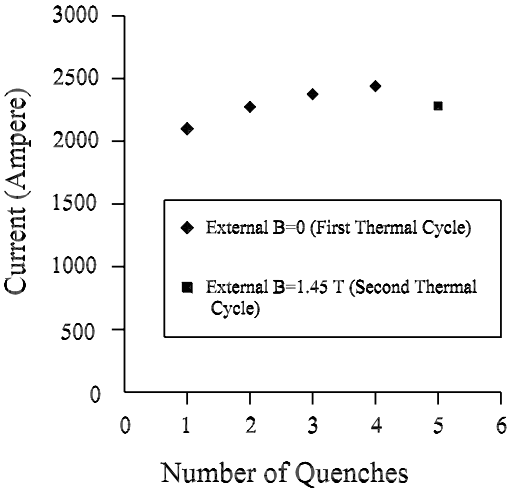

Fig. 21. Training history.

The contribution from the inflector fringe field to the integral field in the storage ring was measured by subtracting the field map with the inflector on from the field map with the inflector off and warm. A Fourier analysis on a circle with radius $R = 45$ mm around the muon central orbit showed that the maximal multipole term is the skew quadrupole with 0.4 ppm amplitude at $R = 45$ mm. All remaining terms have amplitudes of 0.2 ppm or less. Since this residual field is known to high accuracy, the contribution to the magnetic field systematic error for E821 is negligible.

There are several other methods to measure the screening achieved by the superconducting shield. The capacity of the shielding was measured by using multiple samples of the superconducting sheet with different properties, with the minimum value of $J_c = 1200\ \mathrm{A/mm^2}$ (at 1.5 T, 4.2 K, H$\perp$ NbTi layers), mentioned in Section 5. By using $B = \mu_o J_c d$ (where d is 0.15 mm, the total thickness of the NbTi layers), the maximum flux density, which could be shielded, was measured to be 0.26 T at 1.5 T and 5.0 K (the operating condition in the g-2 runs). The maximum leakage field at the inner surface of the shield was estimated as 0.08 to 0.1 T, which was completely blocked by the shield. The power leads and the downstream edge of the shield had minor field leakage into the storage region.

A second measure of the screening is to observe the amount of main field trapped inside the inflector with the inflector turned off, and the main magnet ramped down, leaving the inflector cold. The superconducting shield traps the main field flux at its maximum current density $J_c(B, T)$. One Hall probe was located inside the inflector beam channel near the upstream end (where $R = 7356.5$ mm). With the main field on at 1.45 T, and the inflector off, the probe measures a 1.2 T field. After the main magnet was ramped down, this probe read 0.23 T (computer logged data) and kept this reading for one week, as long as the temperature of the inflector remained below 7 K. The shielding capability is the same as the trapping capability, giving shielding of field on the order of 0.23 to 0.26 T (or 184,000 $\sim$208,000 A/m in magnetic strength H).

Fig. 22 shows the contours of the magnetic field inhomogeneity in the muon storage region, averaged around the ring. Only four contours are shown: 0 ppm, ± 1 ppm, and a very small region of -2 ppm, in this 284,000 cm^3 muon storage volume. As Section 4 stated, due to the residual fringe field, if we were not using a superconducting shield, we would have seen about 80 lines in the integral contour plot (averaged from 1.4% of the leakage field localized within 2° of the ring). If we were using a flux exclusion tube, or an ordinary

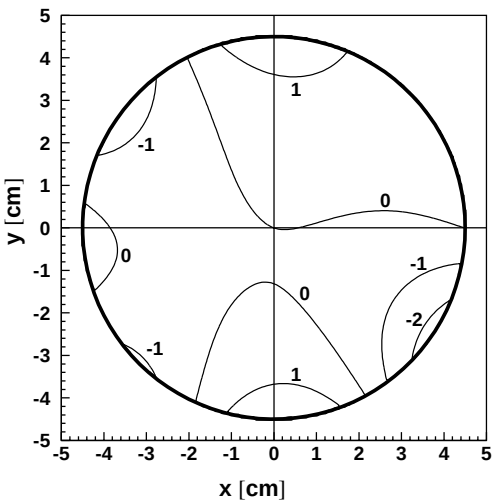

Fig. 22. Muon aperture field uniformity.

DC magnet equivalent, we would have seen more than 500 contours in this plot, provided we could measure the field to such accuracy.

11. Conclusion

A unique and sophisticated superconducting magnet has been developed, which can be used as an injection septum very close to a storage ring. The magnet is optimally compact, and absorbs its own return magnetic flux. Magnetic shielding with superconducting material is successful. The "perfect conductor" property of type II materials has been demonstrated and applied. The fringe field of the device was observed to be at or below a parts per million level, only 23 mm away from a 1.5 T inflector field. The BNL muon g-2 experimental requirements are especially severe and push the technology frontier. This magnet meets the requirements of the experiment, and develops new methods in the construction of accelerator magnets and in the area of applied superconductivity.

Acknowledgements

We thank Dr. Kimura, Dr. Hiyabayashi, and Dr. Mizumachi at KEK, for their strong support of this project.

We thank Furukawa Co. for technical support in several areas and provision of the conductors.

Installation of the inflector into the muon storage ring was a difficult task; we thank John Benante and Don Von Lintig for their state-of-art work. Operations of the inflector involve complicated procedures; we very much appreciate the cryogenic work of Daniel Martin, Mark McNeill, John Stehle, Lou Tenreiro, Emil Varrichio, and Bernard Yatouro of BNL, for their many years dedicated work.

We would like to thank Joe Geller, Tony Curcio and Ron Schroeder of BNL for their critical work on the quench electronics, and Harold Gassner for his simple, clever design on the current ramping device.

Finally, we thank Derek Lowenstein and Phil Pile of the Brookhaven Collider-Accelerator Department for their administrative support and encouragement.

References

[1] J. Bailey, et al., Nucl. Phys. B 100 (1976) 1.
[2] G.T. Danby, et al., Nucl. Instr. and Meth. A 457 (2001) 151.
[3] R. Prigl, et al., Nucl. Instr. and Meth. A 374 (1996) 118.
[4] F. Krienen, private communication.
[5] V. Badea, H.N. Brown, G. Bunce (Chair), G. Cottingham, R. Damm, B. DeVito, F. Krienen, E. Rodger, J. Sandberg, A. Soukas, Pulsed inflector study, g-2 Note, No. 32, October 1989.
[6] F. Krienen, D. Loomba, W. Meng, Nucl. Instr. and Meth. A 283 (1989) 5.
[7] R. Beth, Fields produced by cylindrical current arrays, BNL Internal Report, AADD-102, March 1966.
[8] H. Brown, g-2 Note No. 29, 1989, No. 58, 1990, No. 78, 1991.
[9] H. Brown, G. Bunce, g-2 Note No. 90, 1991.
[10] A. Yamamoto, Nucl. Instr. and Meth. A 453 (2000) 445.
[11] Y. Makida, et al., IEEE Trans. Magn. 27(2) (1991) 1944.
[12] M. Garber, A. Ghosh, W. Samson, IEEE Trans. Magn. 25 (2) (1989) 1940.
[13] Y. Saito, et al., Development of beam inflection superconducting magnet—evaluation of prototype, Tokin Technical Review, No. 20.
[14] W. Meng, K. Woodle, Inflector fringe field study on a wire model, g-2 Note, No. 195, 1994.
[15] A. Yamamoto, Y. Saito, KEK Test results on g-2 SC inflector prototype, g-2 Note, No. 196, 1994.
[16] W. Meng, K. Woodle, BNL Test Results on g-2 Superconducting Inflector Prototype, g-2 Note, No. 209, 1994.
[17] M.N. Wilson, Superconducting Magnets, Oxford Science Publications, Oxford, 1983.
[18] A. Yamamoto, Status of the inflector, Internal Meeting Minutes, 1992;
W. Meng, K. Woodle, Superconducting shield test on g-2 inflector magnet, g-2 Note, No. 210, 1994.
[19] M.A. Green, W. Meng, IEEE Trans. Appl. Supercond. 5 (2) (1995) 667.
[20] G.T. Danby, W. Meng, W. Sampson, K. Woodle, IEEE Trans. Magn. 30 (4) (1994) 1766.
[21] F. Martin, S.J. St. Lorant, W.T. Toner, Nucl. Instr. and Meth. 103 (1972) 503.
[22] C.P. Bean, Phys. Rev. Lett. 8 (6) (1962).
[23] I. Itoh, T. Sasaki, IEEE Trans. Appl. Supercond. 3 (1993) 177.
[24] F. Krienen, et al., IEEE Trans. Appl. Supercond. 5 (2) (1995) 671.
[25] W. Meng, K. Woodle, Superconducting shield test on g-2 inflector prototype, g-2 Note, No. 210, 1994.

[26] L.X. Jia, et al, Cryogenics for the muon g-2 superconducting magnet system, Proceedings of the 15th International Cryogenic Engineering Conference, Genoa, Italy, June 1994, Supplement to Cryogenics, Vol. 34, 1994.
[27] L.X. Jia, et al, Design parameters for gas-cooled electrical leads of the g-2 magnets, Proceedings of the 15th International Cryogenic Engineering Conference, Genoa, Italy, June 1994, Supplement to Cryogenics, Vol. 34, 1994.
[28] A. Yamamoto, et al, First SC inflector for BNL muon g-2 experiment, Proceedings of the 15th International Conference on Magnet Technology, Part 1, Science Press, Beijing, China, 1998, pp. 246–249